

Article

Carbon Sequestration and Landscape Influences in Urban Greenspace Coverage Variability: A High-Resolution Remote Sensing Study in Luohe, China

Jing Huang ¹, Peihao Song ², Xiaojuan Liu ¹, Ang Li ², Xinyu Wang ³, Baoguo Liu ² and Yuan Feng ^{2,*}

¹ School of Life Science, Zhengzhou Normal University, NO. 6 Yingcai Road, Zhengzhou 450004, China; hjing@zznu.edu.cn (J.H.); lxjhenan@zznu.edu.cn (X.L.)

² College of Landscape Architecture and Art, Henan Agricultural University, Zhengzhou 450002, China; peihaos@henau.edu.cn (P.S.); leon_angang@sohu.com (A.L.); liubaoguo-la@henau.edu.cn (B.L.)

³ Institute of Landscape Architecture, Urban Planning and Garden Art, Hungarian University of Agriculture and Life Sciences, 1118 Budapest, Hungary; wang.xinyu@phd.uni-mate.hu

* Correspondence: fy9987@stu.henau.edu.cn

Abstract: Urbanization has significantly altered urban landscape patterns, leading to a continuous reduction in the proportion of green spaces. As critical carbon sinks in urban carbon cycles, urban green spaces play an indispensable role in mitigating climate change. This study aims to evaluate the carbon capture and storage potential of urban green spaces in Luohe, China, and identify the landscape factors influencing carbon sequestration. The research combines on-site data collection with high-resolution remote sensing, utilizing the i-Tree Eco model to estimate carbon sequestration rates across areas with varying levels of greenery. The study reveals that the carbon sequestration capacity of urban green spaces in Luohe City is 1.30 t·C·ha⁻¹·yr⁻¹. Among various vegetation indices, the Enhanced Vegetation Index (EVI) explains urban green space carbon sequestration most effectively through an exponential model ($R^2 = 0.65$, AIC = 136.5). At the city-wide scale, areas with higher greening rates, better connectivity, and more complex edge morphology exhibit superior carbon sequestration efficiency. The explanatory power of key landscape indices on carbon sequestration is 78% across the study area, with variations of 71.5%, 62%, and 84.9% for low, medium, and high greening rate areas, respectively. Moreover, when greening rates reach a certain threshold, maintaining and optimizing the quality of existing green spaces becomes more critical than simply expanding the green area. These insights provide valuable guidance for urban planners and policymakers on enhancing the ecological functions of urban green spaces during urban development.

Keywords: carbon sequestration; urban greenspace; high spatial resolution; Luohe



Citation: Huang, J.; Song, P.; Liu, X.; Li, A.; Wang, X.; Liu, B.; Feng, Y. Carbon Sequestration and Landscape Influences in Urban Greenspace Coverage Variability: A High-Resolution Remote Sensing Study in Luohe, China. *Forests* **2024**, *15*, 1849. <https://doi.org/10.3390/f15111849>

Academic Editor: Jinda Qi

Received: 20 September 2024

Revised: 14 October 2024

Accepted: 18 October 2024

Published: 23 October 2024



Copyright: © 2024 by the authors. Licensee MDPI, Basel, Switzerland. This article is an open access article distributed under the terms and conditions of the Creative Commons Attribution (CC BY) license (<https://creativecommons.org/licenses/by/4.0/>).

1. Introduction

Since the policy of reform and opening up, the process of urbanization in China has accelerated at a remarkable pace [1–3]. Increasing energy consumption and rapid economic growth resulted in a nearly fourfold increase in CO₂ emissions in China between 1980 and 2006. As a consequence, by 2006, China had overtaken the United States in CO₂ emissions, making it the world's leading CO₂ emitter [4]. In recent years, the Chinese government has implemented various CO₂ emission reduction strategies, while significantly expanding urban green spaces due to their numerous environmental benefits and positive impact on human well-being [5,6]. The concept of “forest cities” was introduced as part of this initiative, referring to urban areas that incorporate large-scale afforestation and ecological greening throughout the city to create a holistic urban ecosystem. Statistics show that the number of forest cities in China increased from 22 between 2004 and 2010 to 219 by 2024 [7]. China's National Forest City Development Plan (2018–2025) outlines the goal of establishing national forest cities across six clusters, aiming to reach 200 cities by 2020 and

expand to 300 by 2025 [8]. This initiative provides a valuable opportunity to explore how Chinese urban areas can contribute to addressing future climate change challenges.

Numerous studies indicate that green spaces within cities can sequester substantial amounts of carbon [9–11], making them an effective strategy for offsetting CO₂ emissions [12–14]. The higher carbon sequestration efficiency in urban areas can be attributed to several mechanisms. First, urban green spaces often receive higher levels of nitrogen deposition and CO₂ concentration compared to rural areas, which can stimulate plant growth and enhance photosynthesis [15,16], leading to increased carbon uptake. Additionally, urban heat island effects can extend the growing season for plants in cities, further boosting their carbon sequestration potential [17]. Moreover, urban landscaping practices, such as regular irrigation and fertilization, can maintain healthy vegetation growth, which supports continuous carbon absorption [18]. These factors collectively contribute to a higher rate of carbon sequestration in urban environments compared to non-urban areas. Heath et al. (2011) discovered that although urban forests occupy merely 3% of U.S. land, they are responsible for storing 14% of the carbon from all terrestrial forests [19]. Carbon stored in urban and suburban areas shared about 10% of that in the entire terrestrial ecosystems in the USA [20]. There is a significantly higher carbon density in above-ground biomass in Seattle (USA) than in forests across the country [21]. As compared to natural grasslands, residential grasslands in Baltimore (Baltimore) and Denver (Denver) have a carbon density that is nearly twice as high as that of natural grasslands in the United States [22]. Leicester's above-ground vegetation stored a lot of organic carbon and had a carbon density seven times higher than the national average in Germany [23]. However, previous research concerning the ability of urban green spaces to sequester carbon has primarily focused on measuring the total amount of carbon stored at a given time [24,25], with relatively fewer studies addressing the dynamic process of carbon sequestration [26–28]. In particular, research on how carbon sequestration rates vary across different levels of urban greening remains limited. While some studies have explored the influence of urban characteristics, such as heat island effects or nitrogen deposition, on carbon storage, systematic evaluations of how landscape features—such as greening rate, connectivity, and edge morphology—affect carbon sequestration efficiency are still relatively scarce. Carbon sequestration offers a more accurate and precise measure of the ability of urban vegetation to capture and stabilize atmospheric CO₂, as opposed to simply quantifying the total carbon present at a specific point in time.

This research explored the potential of urban green spaces in Luohe City, China, to sequester carbon. Utilizing on-site surveys, the i-Tree Eco model, and high-resolution imagery, we analyzed how urban green spaces sequester carbon and identified the landscape factors influencing this process. Our aims were threefold: to develop a spatial quantification model for assessing carbon capture in urban green spaces; to identify and assess the contributions of landscape drivers to the carbon sequestration; and to explore strategies for enhancing carbon sequestration through landscape structural adjustments under varying greening rates. By focusing on the dynamic carbon sequestration process and examining various landscape characteristics, this research addresses the relative scarcity of studies in these areas and provides new insights into how different urban landscape features influence carbon sequestration efficiency.

2. Materials and Methods

2.1. Study Area

Luohe City (113°27'–114°16' E, 33°24'–33°59' N), located in the central-southern part of Henan Province, was selected as the study area (Figure 1). The city covers over 2617 km² and consists of three districts (Yancheng, Yuanhui, and Shaoling) and two counties (Wuyang and Linying) [29]. With a population of approximately 2.37 million in 2021, Luohe is a typical mid-sized Chinese city. Situated in a subtropical-to-temperate transitional zone, the city experiences a humid subtropical climate, characterized by an average annual

rainfall of 786 mm and a mean temperature of 14.6 °C, which support a diverse range of native and non-native plant species.

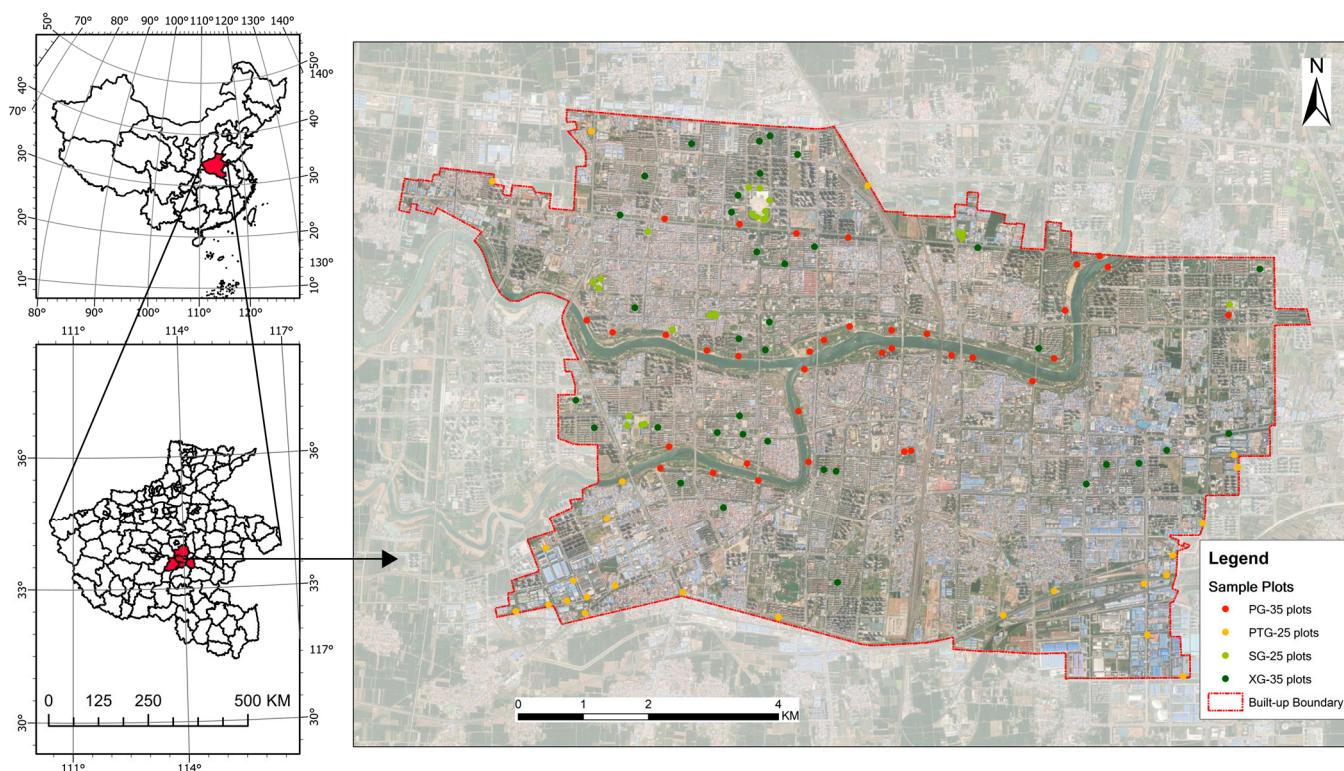


Figure 1. Study area and sample plot distribution across four green space types. (Image captured by Trimble UX5 UAV using RGB bands).

The majority of the rainfall occurs from July to September, accounting for over 80% of the annual precipitation. The city's topography is relatively flat, with an elevation difference of less than 4 m across the entire area. Over the past 30 years, Luohe has undergone rapid population growth and urbanization, similar to many other cities in China [30]. The built-up area is characterized by numerous fragmented and disconnected green spaces scattered throughout the urban districts, which are essential for improving quality of life and addressing ecological challenges associated with urban expansion. Currently, green space and green coverage account for 38.12% and 42.91% of the built-up area, respectively, with per capita public green space reaching approximately 18.1 square meters. These factors contribute to Luohe's reputation as one of the most livable cities in China.

2.2. Remote Sensing Data and Data Processing

This study utilized two types of remote sensing data, including seasonal unmanned aerial vehicle (UAV) images with a high resolution of 9 cm, to analyze land use and the specifics of urban green spaces in the study area. Urban green spaces are categorized into four primary types based on their ecological functions: public parks, protective green spaces, square green spaces, and attached green spaces, as defined by the Standard for Classification of Urban Green Space (CJJ/T85-2017) from the Ministry of Housing and Urban-Rural Development of China. Using leaf-off seasonal UAV images and the Present Land Use Map of Luohe City, the different types of urban green spaces in this study area were analyzed and mapped to determine their spatial distribution. GaoFen-2 (GF-2) data, used for algorithm verification, come from China's first civil optical satellite with sub-meter resolution, launched in 2014. It features both panchromatic and multispectral cameras. The width of each GF-2 image is 45 km. For this study, a GF-2 satellite image from 5 September 2018 was retrieved from <http://www.gscloud.cn> (accessed on 3 June 2024). It was then

processed with ENVI software (version 5.3.1, Harris Corporation, Melbourne, FL, USA), including steps such as radiometric calibration, orthorectification, atmospheric correction, geometrical registration, and image fusion, to produce a multispectral image with four channels (green, blue, red, and NIR) and a spatial resolution of 0.8 m. Seven vegetation indices were employed to analyze vegetation and estimate carbon sequestration within the study area's green spaces, as detailed in the following equation:

$$DVI = NIR - R, \quad (1)$$

$$GNDVI = (NIR - G)/(NIR + G), \quad (2)$$

$$MASVI = 0.5 (2NIR + 1 - \sqrt{(2NIR + 1)^2 - 8(NIR - R)}), \quad (3)$$

$$NDVI = (NIR - R)/(NIR + R), \quad (4)$$

$$RDVI = (NIR - R)/\sqrt{(NIR - R)}, \quad (5)$$

$$RVI = NIR/R, \quad (6)$$

$$EVI = 2.5(NIR - R)/(NIR + 6R - 7.5B + 1), \quad (7)$$

where NIR , R , G , and B represent the reflectivity of the near-infrared (770–890 nm), red (630–690 nm), green (520–590 nm), and blue bands (450–520 nm), respectively. Equations (1)–(7) represent various vegetation indices used to estimate vegetation density, health, and productivity by analyzing different spectral band combinations. The Difference Vegetation Index (DVI) and Normalized Difference Vegetation Index (NDVI) assess vegetation density and health by comparing near-infrared (NIR) and red reflectance. The Green Normalized Difference Vegetation Index (GNDVI) uses green and NIR bands to evaluate chlorophyll concentration. The Modified Atmospherically Resistant Vegetation Index (MASVI) mitigates atmospheric effects on vegetation measurements, while the Renormalized Difference Vegetation Index (RDVI) enhances sensitivity to dense vegetation. The Ratio Vegetation Index (RVI) monitors plant growth through the NIR to red ratio, and the Enhanced Vegetation Index (EVI) improves sensitivity in high biomass areas and reduces atmospheric influence by incorporating the blue band. To minimize bias brought by the non-vegetation part in the sample plot, the average vegetation indices of vegetation space only in each sample plot were extracted.

2.3. Field Survey and Carbon Sequestration Estimation

The i-Tree Eco workbook from the US Forest Service outlines three methods for establishing sample plots in field investigations: layering, random, and grid. The protocol also noted that land stratification could help reveal differences between various land uses [31].

We employed a modified sampling approach using a pre-stratification scheme for different types of urban green spaces. This method provided more accurate samples and vegetation data compared to traditional techniques. ESRI ArcGIS software (version 10.8) was used to generate stratified random sample points exclusively within these green spaces. The corresponding quadrat boundaries were generated by the buffer tool with a radius of about 11.3 m. The following green space strata and sample plots were deployed in this study:

(1) Public parks: These are accessible to the public and include a variety of parks such as comprehensive, community, theme, botanical gardens, belt, and forest parks. (2) Protective green spaces: These areas are generally inaccessible and serve purposes such as ecological isolation and protection. Examples include green belts along highways and railways, power line corridors, and industrial plant buffers. (3) Square green spaces: These publicly accessible areas are used for recreation, events, and disaster prevention, and have a green cover ratio exceeding 35%. (4) Attached green spaces: These are integrated with various land uses, such as residential, commercial, industrial, and public facilities.

A total of 120 circular sample plots, each 404.7 m² as recommended by Nowak [32], were distributed across public parks (35 plots), protective green spaces (25 plots), square green spaces (25 plots), and attached green spaces (35 plots). The number of plots for each green space type was allocated proportionally based on its area and complexity. For each plot, the photos showing the surrounding environment and vegetation inside were taken during field investigation, and we used a modified table for field survey created based on the recommended sample plot data collection sheet. Specifically, data were collected on plot characteristics such as tree and shrub coverage, planted space ratio, and ground cover beneath the canopy. Tree metrics included species, height, DBH, canopy missing percentage, crown size, dieback percentage, and light exposure. For shrubs, information on species, average height, proportion, and mass missing percentage was recorded. Adhering to the i-Tree Eco protocol, field investigations were carried out during the leaf-on season (May to August 2018) to accurately collect sample plot and vegetation data, ensuring proper tree identification and measurement. Plot maps at a 1:500 scale were generated and printed from UAV images, clearly outlining the survey boundaries. Field data were successfully collected from 111 plots, including 35 in public parks, 23 in protective green spaces, 23 in square green spaces, and 33 in attached green spaces, while 9 plots were unachievable and 5 were misclassified. The collected data were then input into i-Tree Eco v6.0 for ecosystem service analysis and assessment of urban green spaces [11,33,34].

2.4. Relationship Between Carbon Sequestration and Landscape Metrics

The landscape index provides highly condensed information about landscape patterns and can be regarded as spatially discontinuous data. Landscape structure composition, spatial configuration, and heterogeneity are reflected in this quantitative index. This study investigates landscape structure, specifically the composition and configuration of built-up land, as a driver of carbon sequestration. The landscape pattern index method is employed to quantitatively assess landscape pattern characteristics using Fragstats 4.2 software [35–37]. Given that blocks typically measure 400 × 400 m² (ranging from 300 × 300 to 500 × 500 m²) and are few, we selected the ¼ block as the smallest analysis unit, dividing the built-up area into a 200 × 200 m² grid to verify the relationship between carbon sequestration and landscape metrics. To assess how landscape structure affects carbon sequestration in urban green spaces at varying greening rates, the built-up areas were categorized into high (≥65%), medium (30% < greening rate < 65%), and low (≤30%) greening areas, following China’s “Specification for Urban Landscaping and Greening Planning and Design” (GB 50420-2007) standards. Moreover, 11 indicators from 5 classifications were selected and calculated for each grid scale (Table 1).

Table 1. Description of landscape indicators.

Classification	Landscape Index	Abbr.	Description
Fragmentation indicator	Number of patches	NP	Represents the total number of distinct patches within a landscape.
	Patch density	PD	Indicates the frequency of patches per unit area, reflecting landscape fragmentation.
Agglomeration indicator	Patch cohesion index	COHESION	Indicates the extent to which similar patches are clustered together.
	Aggregation index	AI	Reflects the spatial clustering of patches of the same type.

Table 1. Cont.

Classification	Landscape Index	Abbr.	Description
Connectivity indicator	Core area mean	CORE_MN	Average size of core areas within patches, important for ecological processes.
	Proportion of like adjacencies	PLADJ	Proportion of a patch's perimeter that is adjacent to the same patch type.
Dominance indicator	Percentage of landscape	PLAND	Percentage of the green spaces.
Shape complexity indicator	Landscape shape index	LSI	Quantifies the complexity of patch shapes in the landscape.
	Normalized landscape shape index	NLSI	Normalizes the shape complexity on a scale from 0 to 1, with higher values indicating more complex shapes.
Dispersion indicator	Landscape division index	DIVISION	Measures the degree to which the landscape is split into isolated patches.
	Effective mesh size	MESH	Assesses the average spacing or distance between patch centroids in the landscape.

3. Results

3.1. Spatial Assessment Model for Carbon Sequestration

The plot of carbon sequestration vs. vegetation indices (VIs) for the 120 plots is shown in Figure 2. The EVI-CS model demonstrated a superior fit with a coefficient of determination (R^2) of 0.65, significantly higher than other models examining the relationship between VIs and carbon sequestration (Table 2). The model's Akaike Information Criterion (AIC) was approximately 136.52, considerably lower than other statistical models, indicating an optimal balance between model complexity and accuracy. Consequently, this study employed EVI as an ideal vegetation index for estimating carbon sequestration in urban green spaces.

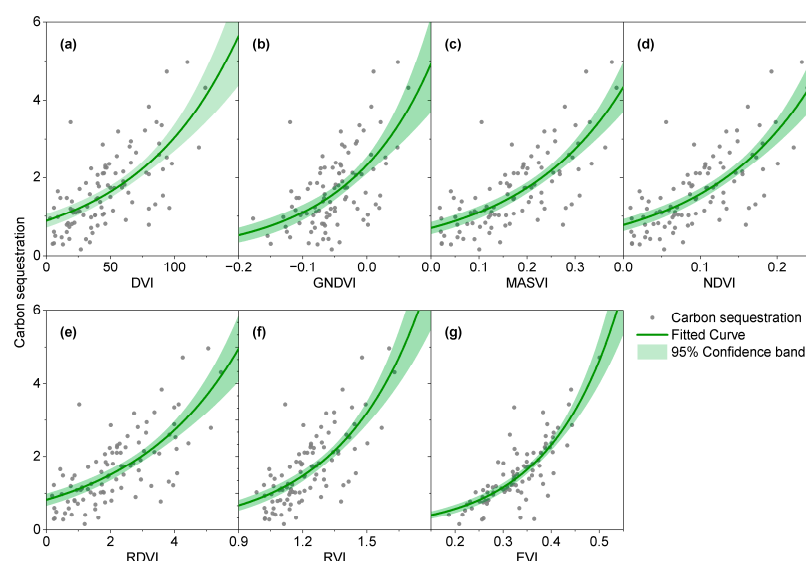


Figure 2. Carbon sequestration ($\text{kg}\cdot\text{C}\cdot\text{pixel}^{-1}$) and scaled VIs for 120 plots. (The solid line represents the final model for carbon storage and the vegetation index). Models (a–g) represent the relationships between carbon sequestration and DVI, GNDVI, MASVI, NDVI, RDVI, RVI, and EVI, respectively.

Table 2. Description of VIs–Carbon sequestration models.

Model	R ²	AIC
$C_{\text{seq}}^1 = e^{0.012\text{DVI}-0.126}$	0.4565	204.6325
$C_{\text{seq}} = e^{7.488\text{GNDVI}-0.843}$	0.3553	221.4447
$C_{\text{seq}} = e^{4.564\text{MASVI}-0.361}$	0.5464	192.7188
$C_{\text{seq}} = e^{7.102\text{NDVI}-0.256}$	0.5456	193.3446
$C_{\text{seq}} = e^{0.299\text{RDVI}-0.193}$	0.5043	198.8507
$C_{\text{seq}} = e^{2.595\text{RVI}-2.73}$	0.5415	194.5988
$C_{\text{seq}} = e^{6.932\text{EVI}-1.934}$	0.6484	136.5168

¹ C_{seq} refers to carbon sequestration.

3.2. Overview of Urban Trees and Carbon Sequestration

This survey examined a total of 1496 individual plants, covering 69 unique species of urban trees across 41 families and 52 genera. Notable species include Chinese Privet (*Ligustrum lucidum*), Golden Rain Tree (*Koelreuteria paniculata*), Japanese Cherry (*Prunus serrulata*), Ginkgo (*Ginkgo biloba*), Sweet Olive (*Osmanthus fragrans*), Chinese Photinia (*Photinia serratifolia*), and Crepe Myrtle (*Lagerstroemia indica*) (Figure 3a). The ratio of evergreen to deciduous trees is roughly 1.9:1, and the ratio of woody shrubs to trees is about 1.4:1. Of the 47 tree species assessed, 45% are evergreen and 55% are deciduous. The tree species include 16 flowering varieties and 9 with colored foliage. Among the 26 shrub species, 65% are evergreen and 35% are deciduous, including 10 ornamental flowering types and 9 with colored foliage.

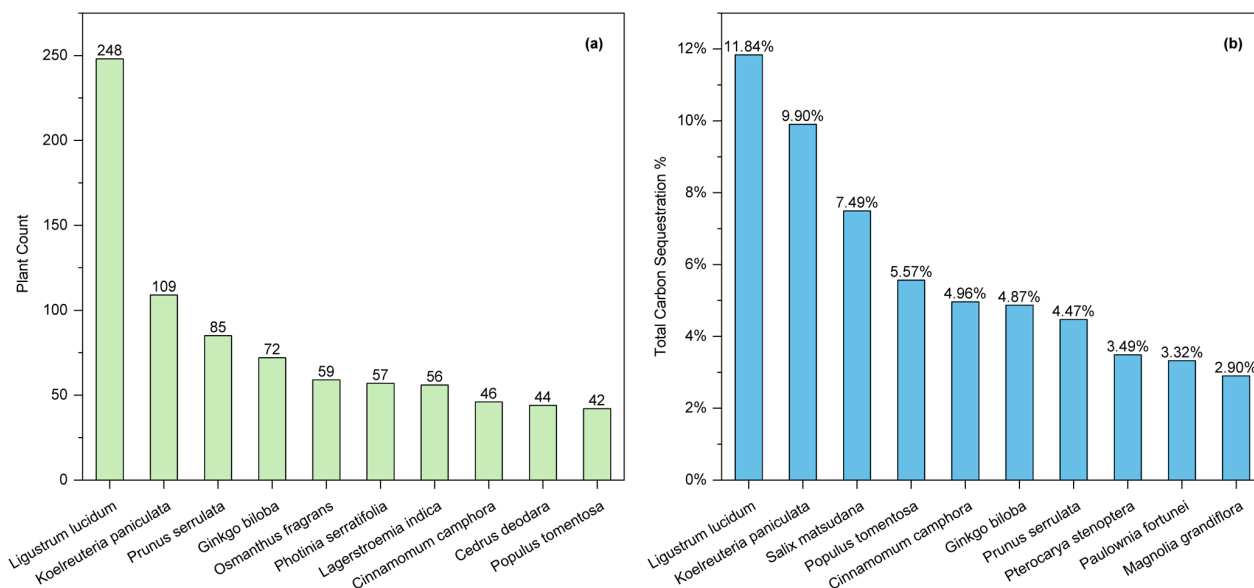


Figure 3. (a) Dominant species; (b) dominant species of carbon sequestration.

Chinese Privet, Golden Rain Tree, and Chinese Willow (*Salix matsudana*) are the dominant tree species for carbon sequestration, accounting for 11.84%, 9.90%, and 7.49% of the annual carbon sequestration of trees in Luoyang, respectively (Figure 3b). Notably, *Salix matsudana*, despite being one of the top contributors to carbon sequestration, has only 32 individual trees. Spatially, the carbon sequestration capacity of green spaces in Luohe is significantly affected by urbanization, exhibiting notable spatial clustering. The average annual carbon sequestration efficiency per tree for Empress Tree (*Paulownia fortunei*), Chinese Willow, Chinese Wingnut (*Pterocarya stenoptera*), Chinese Tallow (*Sapium sebiferum*), Siberian Elm (*Ulmus pumila*), and Chinese Hackberry (*Celtis sinensis*) exceeds 10 kg per year, with values reaching 21.91, 16.97, 12.65, 11.43, 11.20, and 10.52 kg per year, respectively.

In the study area, green space carbon sequestration was highly variable and significantly impacted by urban development, showing regional clustering (Figure 4). Carbon sequestration in green spaces varied from 0.14 to 2.30 $\text{t}\cdot\text{C}\cdot\text{ha}^{-1}\cdot\text{yr}^{-1}$, with an average of 1.30 $\text{t}\cdot\text{C}\cdot\text{ha}^{-1}\cdot\text{yr}^{-1}$. Notably, the majority of carbon sequestration occurred within the 0.14 – 1.05 $\text{t}\cdot\text{C}\cdot\text{ha}^{-1}\cdot\text{yr}^{-1}$ range. In the city's outskirts, especially to the southeast, some green space patches showed higher sequestration rates, peaking at 2.30 $\text{t}\cdot\text{C}\cdot\text{ha}^{-1}\cdot\text{yr}^{-1}$.



Figure 4. Spatial distribution of carbon sequestration in green space of Luohe City.

3.3. Relationship Between Carbon Sequestration and Greenery Coverage

In this study, based on UAV and GF-2 estimations, an overall increasing trend in carbon density is observed with the augmentation of urban green coverage (Figure 5). The supplementary plot on the right side of Figure 5 and Table 3 further elucidates the correlation between carbon storage and green coverage, delineated at 95% intervals. The model accuracy, as denoted by the coefficient of determination (R^2), for the maximum and mean carbon densities in relation to varying green coverage attains values of 0.7331 and 0.7099, respectively. However, the minimum carbon density demonstrates an R^2 value of merely 0.2528, which lacks statistical significance and is consequently omitted from subsequent considerations. On average, carbon density tends to increase in tandem with escalating green coverage. Notably, when green coverage surpasses 60%, carbon density displays a heightened amplitude of fluctuation relative to the increase in green coverage. The estimation model suggests that, as green coverage exceeds 60%, the growth trend of maximum and mean carbon densities gradually attenuates and tends toward inverse growth. Moreover, the zenith of carbon storage for both maximum and mean values is reached at urban green coverage levels of 88% and 85%, respectively, after which a descending trajectory becomes evident.

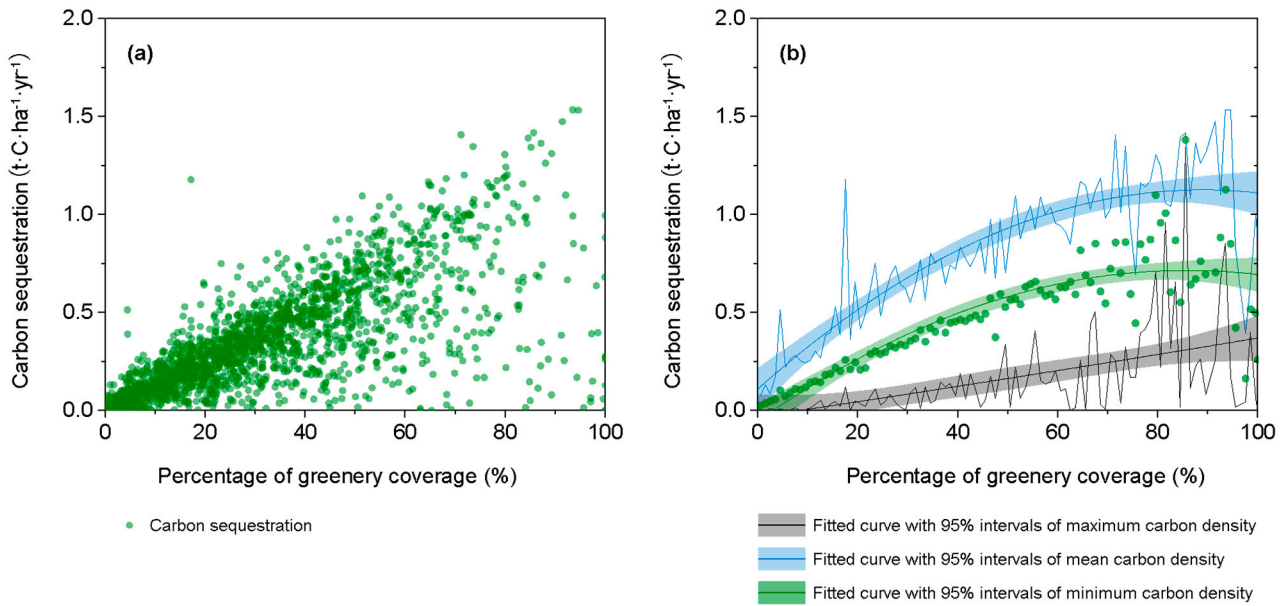


Figure 5. (a) represents the relationship between greenery coverage and carbon sequestration. (b) represents the relationship between varying greenery coverage and the maximum, mean, and minimum carbon densities.

Table 3. The relationship model between carbon sequestration and percentage of greenery coverage.

Carbon Density	Model	R ²	F-Value	p-Value
Maximum carbon density	$C_{seq} = -1.283 \cdot 10^{-4} \cdot P^2 + 0.023 \cdot P - 0.110$	0.733	17.577	<0.001
Mean carbon density	$C_{seq} = -1.046 \cdot 10^{-4} \cdot P^2 + 0.018 \cdot P - 1.046$	0.710	135.607	<0.001
Minimum carbon density	$C_{seq} = 2.171 \cdot 10^{-6} \cdot P^2 + 0.004 \cdot P - 0.031$	0.253	120.904	<0.001

* C_{seq} refers to carbon sequestration.

3.4. Relationship Between Carbon Sequestration and Landscape Structure

The heat map reveals significant variations in how carbon stock density correlates with landscape metrics across different greening rates ($p < 0.05$) (see Figure 6). Notably, the link between carbon sequestration and landscape metrics is stronger in areas with low greening rates compared to those with high greening rates. Across the study area, carbon sequestration is strongly positively correlated with PLAND, PLADJ, MESH, and AI, showing correlation coefficients of 0.73, 0.63, and 0.60 (for both MESH and AI). In contrast, it exhibits significant negative correlations with DIVISION and NLSI, with coefficients of -0.52 and -0.32 , respectively.

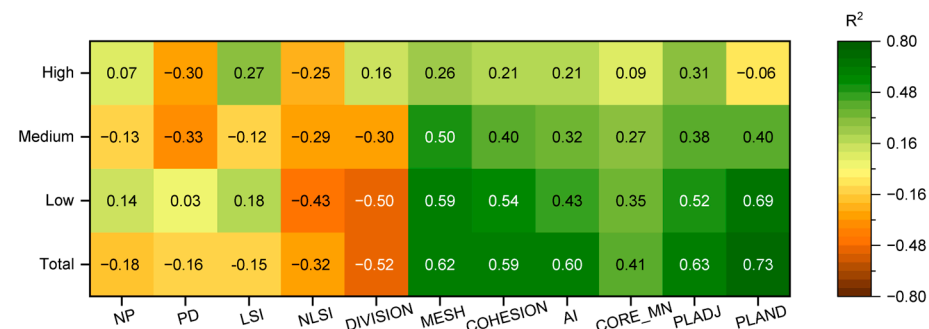


Figure 6. Correlation analysis between carbon sequestration and landscape indices.

Specifically, PLAND, MESH, and PLADJ exhibit the strongest positive correlations with carbon stock in low, medium, and high greening rate areas, with correlation coefficients

of 0.69, 0.50, and 0.31, respectively. Meanwhile, DIVISION shows the strongest negative correlation with carbon stock in low greening rate areas, whereas PD demonstrates the most negative correlations in medium and high greening rate areas, with coefficients of -0.33 and -0.30 , respectively.

3.5. Relative Importance of Landscape Indices

Figure 7 illustrates the primary landscape indices that influence urban carbon sequestration across different greening rates. The height of the bars represents the overall explanatory power of these key landscape indices in explaining changes in carbon sequestration for each greening rate category. The explanatory power is 0.78 for the entire study area and 0.715, 0.62, and 0.849 for low, medium, and high greening rate areas, respectively.

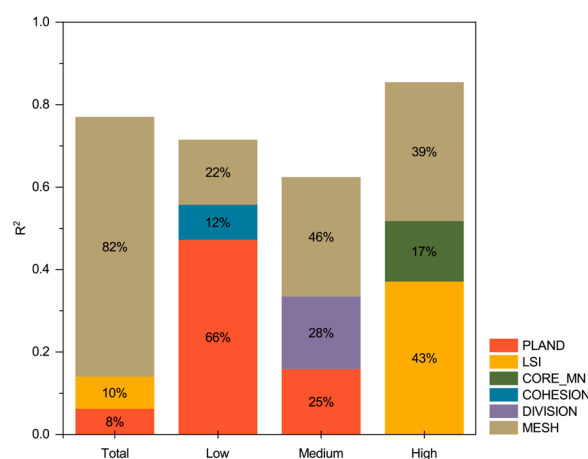


Figure 7. Relative importance of key landscape indices under different greening rates.

For the entire study area, MESH has the greatest impact on changes in carbon stock, with a relative explanatory power of 82%, significantly higher than that of LSI (10.1%) and PLAND (8.1%). MESH also remains the most influential factor in areas with medium greening rates, holding a relative explanatory power of 46%. However, in areas with low and high greening rates, PLAND (66%) and LSI (43%) surpass MESH in relative importance, becoming the dominant factors affecting carbon sequestration.

3.6. The Partial Dependence Analysis of Landscape Indices

This study conducted partial dependence analysis on key landscape indices (Figure 8). Across the entire study area, without considering greening rates, carbon sequestration exhibits a generally monotonic positive relationship with PLAND, MESH, and LSI. When PLAND reaches 65.5, MESH reaches 1.5, and LSI reaches 8, the marginal effects of these landscape indices on carbon sequestration diminish, and the growth in carbon sequestration plateaus.

In low-greening-rate areas, carbon sequestration also shows a monotonic positive relationship with MESH, COHESION, and PLAND, but with distinct growth rates. When MESH is below 0.1, carbon sequestration increases sharply with MESH, then stabilizes. At lower levels of COHESION, carbon sequestration remains stable until COHESION reaches 94, after which it spikes as COHESION increases further. Additionally, the relationship between carbon sequestration and PLAND follows a fluctuating linear pattern, with carbon sequestration showing some variability as PLAND increases. In medium-greening-rate areas, carbon sequestration increases positively with PLAND and MESH. However, as DIVISION grows, carbon sequestration initially decreases and then sharply increases once DIVISION reaches 0.9. In high-greening-rate areas, carbon sequestration exhibits a rapid increase with rising LSI, CORE_MN, and MESH, followed by stabilization. This suggests that in high-greening-rate areas, carbon sequestration is more sensitive to these landscape indices, but the growth effect diminishes once certain levels are reached.

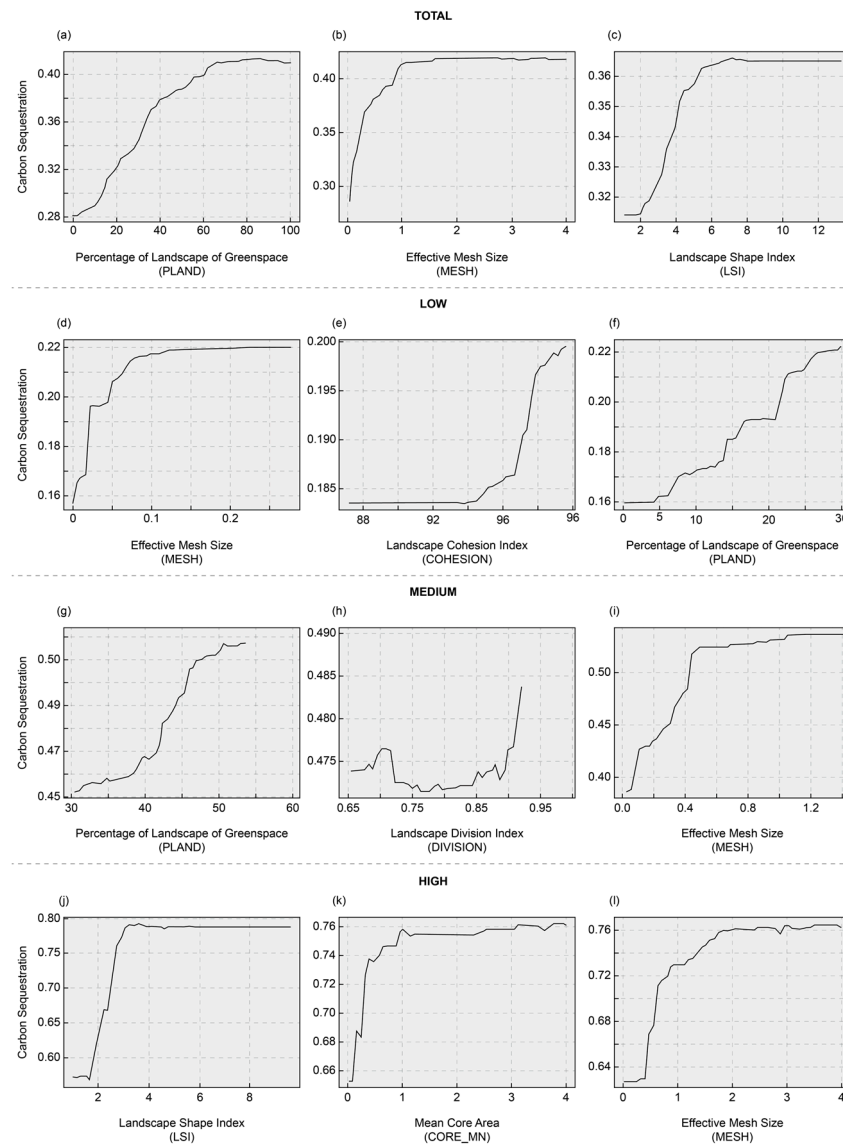


Figure 8. The marginal effects of key landscape indices under different greening rates. (a–c) show the partial dependence of key factors affecting carbon sequestration without considering greenery coverage; (d–f) under low coverage; (g–i) under medium coverage; and (j–l) under high coverage.

4. Discussion

4.1. Comparison with Other Studies

Our results show that urban green spaces in Luohe sequester carbon at a medium rate of $1.30 \text{ t}\cdot\text{C}\cdot\text{ha}^{-1}\cdot\text{yr}^{-1}$, which is higher than that of cities such as Xiamen, Dalian, Urumqi, Yinchuan, Hohhot, Tianjin, Guiyang, Xi'an, Hefei, and Shijiazhuang [38–41], but lower than that of cities such as Shanghai, Nanjing, Hangzhou, Changsha, Chongqing, Guizhou, Ningbo, Wuhan, and Zhengzhou [42–45]. When compared internationally, the carbon sequestration rate in Luohe is higher than the average for certain regions in Canada, which is reported to be $0.574 \pm 0.092 \text{ t}\cdot\text{C}\cdot\text{ha}^{-1}\cdot\text{yr}^{-1}$ [46]. However, it is lower than the average rate in the United States, where Nowak et al. found that urban areas sequester carbon at an average rate of $2.77 \text{ t}\cdot\text{C}\cdot\text{ha}^{-1}\cdot\text{yr}^{-1}$, with significant variation from $1.68 \text{ t}\cdot\text{C}\cdot\text{ha}^{-1}\cdot\text{yr}^{-1}$ in Alaska to $5.81 \text{ t}\cdot\text{C}\cdot\text{ha}^{-1}\cdot\text{yr}^{-1}$ in Hawaii [47]. Additionally, a study in South Korea indicated that carbon sequestration rates in urban areas range from 1.60 to $3.91 \text{ t}\cdot\text{C}\cdot\text{ha}^{-1}\cdot\text{yr}^{-1}$, which places Luohe at the lower end of this range [48]. The possible reasons for these differences are as follows.

First, these differences are likely due to variations in urban tree cover [11]. Using high-resolution imagery (SPOT/ALOS), Zhou et al. (2018) studied urban green spaces in nine cities across China and found that the green coverage rates in Nanjing and Hangzhou were 49.0% and 47.6% [49], respectively, which are higher than those in Tangshan (15.8%) and Tianjin (26.6%). Correspondingly, the carbon sequestration rates of urban green spaces in Nanjing and Hangzhou are $2.87 \text{ t}\cdot\text{C}\cdot\text{ha}^{-1}\cdot\text{yr}^{-1}$ and $1.66 \text{ t}\cdot\text{C}\cdot\text{ha}^{-1}\cdot\text{yr}^{-1}$, respectively, which are higher than those in Tangshan ($1.26 \text{ t}\cdot\text{C}\cdot\text{ha}^{-1}\cdot\text{yr}^{-1}$) and Tianjin ($1.07 \text{ t}\cdot\text{C}\cdot\text{ha}^{-1}\cdot\text{yr}^{-1}$) [42].

Second, natural factors may also play a role. Lower carbon sequestration rates in green spaces are typically observed in northern cities of China, while southern cities tend to have higher rates. For instance, the average annual temperature and precipitation in Nanjing ($15.4 \text{ }^\circ\text{C}$ and 1106.5 mm) and Hangzhou ($17.8 \text{ }^\circ\text{C}$ and 1454 mm) are significantly higher than those in Luohe ($14.6 \text{ }^\circ\text{C}$ and 786 mm), Tangshan ($12.5 \text{ }^\circ\text{C}$ and 600 mm), and Tianjin ($13.4 \text{ }^\circ\text{C}$ and 571 mm). The study by Hong et al. (2024) indicates that surface temperature and elevation are key factors influencing the spatial distribution of carbon sequestration in urban forests.

Third, the differences might be attributed to sampling methods [50]. For example, Shi Yan et al. (2013) assessed the carbon sequestration of urban trees across major cities in China using the tree core method, which involved fewer tree species, all of which were mature trees, potentially leading to an overestimation of carbon sequestration [39]. In contrast, our study employed the i-Tree Eco model, which integrates field survey data with modeling techniques, to estimate carbon sequestration across Luohe's urban green spaces, potentially enhancing the accuracy of our results.

Fourth, human factors also affect the spatial distribution of carbon sequestration. The study by Hong et al. (2024) shows that urban area and population density are major factors influencing the spatial distribution of carbon sequestration, both of which are negatively correlated with carbon sequestration [50]. Higher GDP in built-up areas allows for greater investment in improving the ecological environment by the government. Additionally, human activities can lead to the fragmentation of urban green landscapes, and land use has a significant impact on carbon sequestration.

Therefore, to more accurately quantify the carbon sequestration capacity of urban green spaces and to better understand how urbanization drives changes in carbon sequestration, it is necessary to conduct studies on a smaller scale, such as at the urban landscape level. This would provide a basis for local governments to formulate effective urban management strategies and planning.

4.2. Landscape Structure Drivers of Carbon Sequestration

Urban green spaces are crucial components of landscape patterns that significantly impact carbon sequestration [51,52]. Our study reveals that various landscape structure indices, including PLAND, LSI, and MESH, have different effects on carbon sequestration depending on the greening rates of urban areas [53]. Here, we discuss the possible reasons behind these findings.

First, in areas with low to medium greening rates, a significant positive correlation was found between carbon sequestration capacity and PLAND. This relationship occurs because, in less densely vegetated areas, expanding green space directly increases the amount of vegetation available for carbon sequestration [54,55]. Vegetation in these regions is often less mature or sparse, so any increase in green space can lead to substantial gains in carbon storage through photosynthesis and improvements in local microclimates, which also contribute to increased soil organic carbon. This suggests that in areas with limited green cover, expanding green space is a highly effective strategy for boosting carbon sequestration.

Second, as greening rates increase, the influence of PLAND on carbon sequestration diminishes, and other landscape indices such as LSI [56–58] and CORE_MN become more significant. In high greening rate areas, the complexity of landscape shapes, as measured by LSI, becomes more important because complex, irregular edges of green

patches can enhance edge effects. These edge effects may increase the exposure of plants to sunlight and air, thereby enhancing photosynthetic activity and, consequently, carbon sequestration. Similarly, CORE_MN reflects the size of core areas within landscape patches, where environmental conditions are more stable and disturbances are minimized. Larger core areas provide better conditions for sustained plant growth, leading to more efficient carbon storage. This shift in importance from PLAND to LSI and CORE_MN as greening rates increase likely reflects the saturation of basic carbon sequestration capacity, where further improvements rely more on optimizing the structure and quality of existing green spaces rather than simply expanding them [59].

Third, landscape connectivity, as indicated by MESH, consistently plays a crucial role in enhancing carbon sequestration across all levels of greening rates. The strong positive correlation between MESH and carbon sequestration can be attributed to the fact that larger and more connected green patches facilitate the movement of species, nutrients, and energy across the landscape [60]. This connectivity helps maintain ecological processes and supports more robust plant growth, which in turn enhances carbon sequestration [61]. Additionally, better-connected green spaces can reduce the fragmentation of habitats, which is often associated with reduced carbon efficiency [62,63]. Thus, the consistent importance of MESH across different greening rates underscores the need to design urban landscapes that promote connectivity to maximize carbon sequestration.

Lastly, our study highlights a diminishing marginal effect on carbon sequestration as green space area, connectivity, and shape complexity increase. This phenomenon suggests that beyond a certain point, the carbon sequestration capacity of green spaces begins to stabilize, likely due to ecological saturation. As green spaces become more mature and well connected, the ecosystem's capacity to sequester additional carbon may reach its natural limit, where additional green space or further increases in connectivity or shape complexity yield only minimal gains. This stabilization could be due to the fact that plant growth and carbon sequestration processes within the ecosystem have reached their maximum efficiency. Therefore, in highly vegetated urban areas, the focus should shift from expanding green spaces to maintaining and enhancing the quality and health of existing green spaces to sustain their carbon sequestration potential.

4.3. Implications and Outlook for the Future

For low-greening-rate urban patches, the key to enhancing carbon sequestration capacity lies in increasing green space area and improving connectivity. Urban renewal projects can convert idle or abandoned land into green spaces, or require green space construction in new development areas [64]. Additionally, establishing greenways and ecological corridors to connect existing green patches and reduce fragmentation can effectively enhance the overall connectivity of the ecological network [65,66]. Meanwhile, ecological restoration measures, such as soil remediation and replanting native vegetation, can improve the quality and health of green spaces in low-greening-rate areas [67], thereby significantly boosting carbon sequestration capacity [68]. These strategies, supported by government policies and public participation, can improve ecological benefits while enhancing the overall environmental quality of the city, providing crucial support for sustainable urban development.

In medium-greening-rate urban patches, carbon sequestration capacity can be significantly enhanced by reducing landscape fragmentation and improving connectivity. Specifically, planning and constructing greenways and ecological corridors can connect dispersed green patches, reducing the distance between them and improving overall landscape connectivity. Additionally, optimizing the internal structure of green spaces by introducing water bodies, wetlands [69,70], and vegetation buffers [71] can enhance ecological functions. Further measures include introducing diverse native plant species, particularly those with strong carbon sequestration capabilities [72]. These actions can be implemented through local government green infrastructure projects or community greening initiatives,

thereby strengthening the health of ecosystems and enhancing the carbon sink function of green spaces [73].

In high-greening-rate urban patches, although the carbon sequestration function of green spaces is already significant, there is still room for improvement. First, optimizing the shape of green spaces can effectively enhance edge effects. For example, designing winding paths and irregular boundaries along green space edges can maximize carbon sequestration efficiency in edge areas. Moreover, expanding core areas within green spaces, such as reducing paved surfaces or redesigning the layout, can reduce edge disturbances and provide a more stable ecological environment, thereby improving overall carbon sequestration. Furthermore, maintaining and managing the quality and diversity of existing green spaces is equally essential. Regular soil improvement and plant health monitoring can ensure biodiversity and healthy growth, further enhancing carbon sequestration capacity [74]. In practice, these optimization measures can be promoted through urban planning policies, such as encouraging community involvement in green space maintenance or introducing more complex green space designs in public projects.

5. Conclusions

This study aimed to evaluate the carbon sequestration potential of urban green spaces in Luohe, China, and to identify the landscape factors that influence this process. Using field surveys, the i-Tree Eco model, and high-resolution remote sensing data, we set out to develop a spatial quantification model for carbon capture and explore strategies for optimizing urban greening to enhance carbon sequestration. The findings demonstrate that Luohe's urban green spaces sequester an average of $1.30 \text{ t}\cdot\text{C}\cdot\text{ha}^{-1}\cdot\text{yr}^{-1}$, with substantial spatial variability influenced by landscape characteristics such as greening coverage, connectivity, and shape complexity. The Enhanced Vegetation Index (EVI) proved to be the most reliable predictor of carbon sequestration, underscoring the link between vegetation health and carbon capture potential.

The analysis revealed that different landscape features had varying degrees of impact depending on the greening rates. In areas with low to medium greening, patch size and connectivity (PLAND and MESH) were the strongest predictors, while shape complexity (LSI) and core area size (CORE_MN) were more significant in high-greening areas. These results suggest that once a certain greening threshold is reached, improving the structural quality of green spaces becomes more effective than expanding their area.

Comparatively, Luohe's sequestration rate is higher than that of many northern Chinese cities but lower than in southern regions. Internationally, it exceeds the average for some regions in Canada but is below the U.S. average, reflecting differences in climate, urban tree cover, and methodological approaches.

The study's goal to provide actionable insights for urban planners is supported by these findings, which highlight the need to tailor greening strategies based on local conditions. In areas with low greening, expanding green space and enhancing connectivity should be prioritized, while in high-greening areas, efforts should focus on optimizing the quality and structural complexity of existing green spaces. Future research should explore the long-term dynamics of urban carbon sequestration and incorporate additional factors, such as soil properties and species diversity, to improve the accuracy of estimates. These insights lay a foundation for targeted strategies to maximize the ecological benefits of urban green spaces, contributing to climate change mitigation and sustainable urban development.

Author Contributions: Conceptualization, J.H., X.W. and B.L.; data curation, P.S., X.L., Y.F. and B.L.; formal analysis, J.H., P.S., X.L. and Y.F.; funding acquisition, A.L. and B.L.; investigation, X.L., A.L., X.W. and B.L.; methodology, A.L., X.W. and Y.F.; project administration, J.H., P.S. and X.L.; resources, J.H., A.L. and X.W.; supervision, P.S., X.L. and B.L.; validation, P.S., A.L. and B.L.; visualization, A.L. and Y.F.; writing—original draft, J.H., P.S. and Y.F.; writing—review and editing, X.W. and Y.F. All authors have read and agreed to the published version of the manuscript.

Funding: This research was funded by “the Key Research and Development Special Program of Henan Province, grant number 241111211500”, “the Technology Research and Development Program of Henan Province, grant number 242102320330 and 242102320320” and “the Special Fund for Young Talents at Henan Agricultural University, grant number 30501053”.

Data Availability Statement: The raw data supporting the conclusions of this article will be made available by the authors on request.

Conflicts of Interest: The authors declare no conflicts of interest.

References

- Huang, X.; Xia, J.; Xiao, R.; He, T. Urban Expansion Patterns of 291 Chinese Cities, 1990–2015. *Int. J. Digit. Earth* **2019**, *12*, 62–77. [CrossRef]
- Gong, P.; Li, X.; Zhang, W. 40-Year (1978–2017) Human Settlement Changes in China Reflected by Impervious Surfaces from Satellite Remote Sensing. *Sci. Bull.* **2019**, *64*, 756–763. [CrossRef]
- Peng, J.; Lin, H.; Chen, Y.; Blaschke, T.; Luo, L.; Xu, Z.; Hu, Y.; Zhao, M.; Wu, J. Spatiotemporal Evolution of Urban Agglomerations in China during 2000–2012: A Nighttime Light Approach. *Landsc. Ecol.* **2020**, *35*, 421–434. [CrossRef]
- Bilgili, F.; Mugaloglu, E.; Koçak, E. The Impact of Oil Prices on CO₂ Emissions in China: A Wavelet Coherence Approach. In *Econometrics of Green Energy Handbook: Economic and Technological Development*; Shahbaz, M., Balsalobre-Lorente, D., Eds.; Springer International: Cham, Switzerland, 2020; pp. 31–57. ISBN 978-3-030-46847-7.
- Zhou, W.; Wang, J.; Cadenasso, M.L. Effects of the Spatial Configuration of Trees on Urban Heat Mitigation: A Comparative Study. *Remote Sens. Environ.* **2017**, *195*, 1–12. [CrossRef]
- Kuang, W.; Zhang, S.; Li, X.; Lu, D. A 30-Meter Resolution National Urban Land-Cover Dataset of China, 2000–2015. *Earth Syst. Sci. Data Discuss.* 2019; preprint. [CrossRef]
- PRC. Investing in Forest Cities. Available online: https://www.gov.cn/yaowen/liebiao/202404/content_6944811.htm (accessed on 1 July 2024).
- China Daily. China to Have 300 Forest Cities by 2025. Available online: http://english.scio.gov.cn/chinavoices/2018-07/09/content_55763384.htm (accessed on 1 August 2023).
- Zhao, S.; Zhu, C.; Zhou, D.; Huang, D.; Wemer, J. Organic Carbon Storage in China’s Urban Areas. *PLoS ONE* **2013**, *8*, e71975. [CrossRef]
- Nowak, D.J.; Greenfield, E.J. US Urban Forest Statistics, Values, and Projections. *J. For.* **2018**, *116*, 164–177. [CrossRef]
- Yuan, Y.; Guo, W.; Tang, S.; Zhang, J. Effects of Patterns of Urban Green-Blue Landscape on Carbon Sequestration Using XGBoost-SHAP Model. *J. Clean. Prod.* **2024**, *476*, 143640. [CrossRef]
- Dorendorf, J.; Eschenbach, A.; Schmidt, K.; Jensen, K. Both Tree and Soil Carbon Need to Be Quantified for Carbon Assessments of Cities. *Urban. For. Urban. Green.* **2015**, *14*, 447–455. [CrossRef]
- Ren, Z.; Zheng, H.; He, X.; Zhang, D.; Shen, G.; Zhai, C. Changes in Spatio-Temporal Patterns of Urban Forest and Its above-Ground Carbon Storage: Implication for Urban CO₂ Emissions Mitigation under China’s Rapid Urban Expansion and Greening. *Environ. Int.* **2019**, *129*, 438–450. [CrossRef]
- Yu, C.; Wang, Q.; Zhang, S.; Zeng, H.; Chen, W.; Chen, W.; Lou, H.; Yu, W.; Wu, J. Effects of Strigolactone on *Torreya Grandis* Gene Expression and Soil Microbial Community Structure Under Simulated Nitrogen Deposition. *Front. Plant Sci.* **2022**, *13*, 908129. [CrossRef]
- Keenan, T.F.; Hollinger, D.Y.; Bohrer, G.; Dragoni, D.; Munger, J.W.; Schmid, H.P.; Richardson, A.D. Increase in Forest Water-Use Efficiency as Atmospheric Carbon Dioxide Concentrations Rise. *Nature* **2013**, *499*, 324–327. [CrossRef]
- Pretzsch, H.; Biber, P.; Uhl, E.; Dahlhausen, J.; Schütze, G.; Perkins, D.; Rötzer, T.; Caldentey, J.; Koike, T.; van Con, T.; et al. Climate Change Accelerates Growth of Urban Trees in Metropolises Worldwide. *Sci. Rep.* **2017**, *7*, 15403. [CrossRef] [PubMed]
- Gavali, R.S.; Shaikh, H.M.Y. Estimation of Carbon Storage in the Tree Growth of Solapur University Campus, Maharashtra, India. *Int. J. Sci. Res.* **2016**, *5*, 2364–2367. [CrossRef]
- Heath, L.S.; Smith, J.E.; Skog, K.E.; Nowak, D.J.; Woodall, C.W. Managed Forest Carbon Estimates for the US Greenhouse Gas Inventory, 1990–2008. *J. For.* **2011**, *109*, 167–173. [CrossRef]
- Churkina, G.; Brown, D.G.; Keoleian, G. Carbon Stored in Human Settlements: The Conterminous United States. *Glob. Change Biol.* **2010**, *16*, 135–143. [CrossRef]
- Hutyra, L.R.; Duren, R.; Gurney, K.R.; Grimm, N.; Kort, E.A.; Larson, E.; Shrestha, G. Urbanization and the Carbon Cycle: Current Capabilities and Research Outlook from the Natural Sciences Perspective. *Earth’s Future* **2014**, *2*, 473–495. [CrossRef]
- Pouyat, R.V.; Yesilonis, I.D.; Golubiewski, N.E. A Comparison of Soil Organic Carbon Stocks between Residential Turf Grass and Native Soil. *Urban. Ecosyst.* **2009**, *12*, 45–62. [CrossRef]
- Davies, Z.G.; Edmondson, J.L.; Heinemeyer, A.; Leake, J.R.; Gaston, K.J. Mapping an Urban Ecosystem Service: Quantifying above-Ground Carbon Storage at a City-Wide Scale. *J. Appl. Ecol.* **2011**, *48*, 1125–1134. [CrossRef]
- Sun, Y.; Xie, S.; Zhao, S. Valuing Urban Green Spaces in Mitigating Climate Change: A City-Wide Estimate of Aboveground Carbon Stored in Urban Green Spaces of China’s Capital. *Glob. Change Biol.* **2019**, *25*, 1717–1732. [CrossRef]

24. Helen; Jarzebski, M.P.; Gasparatos, A. Land Use Change, Carbon Stocks and Tree Species Diversity in Green Spaces of a Secondary City in Myanmar, Pyin Oo Lwin. *PLoS ONE* **2019**, *14*, e0225331. [[CrossRef](#)]
25. Dong, L.; Wang, Y.; Ai, L.; Cheng, X.; Luo, Y. A Review of Research Methods for Accounting Urban Green Space Carbon Sinks and Exploration of New Approaches. *Front. Environ. Sci.* **2024**, *12*, 1350185. [[CrossRef](#)]
26. Jin, S.; Zhang, E.; Guo, H.; Hu, C.; Zhang, Y.; Yan, D. Comprehensive Evaluation of Carbon Sequestration Potential of Landscape Tree Species and Its Influencing Factors Analysis: Implications for Urban Green Space Management. *Carbon. Balance Manag.* **2023**, *18*, 17. [[CrossRef](#)] [[PubMed](#)]
27. Lv, H.; Wang, W.; He, X.; Wei, C.; Xiao, L.; Zhang, B.; Zhou, W. Association of Urban Forest Landscape Characteristics with Biomass and Soil Carbon Stocks in Harbin City, Northeastern China. *PeerJ* **2018**, *6*, e5825. [[CrossRef](#)]
28. Henan Provincial Bureau of Statistics. Henan Statistical Yearbook 2023. Available online: <https://oss.henan.gov.cn/sbgt-wztipt/attachment/hntjj/hntj/lib/tjnj/2023nj/zk/indexch.htm> (accessed on 1 July 2024).
29. Zhu, X.; Li, Y.; Zhang, P.; Wei, Y.; Zheng, X.; Xie, L. Temporal–Spatial Characteristics of Urban Land Use Efficiency of China’s 35mega Cities Based on DEA: Decomposing Technology and Scale Efficiency. *Land. Use Policy* **2019**, *88*, 104083. [[CrossRef](#)]
30. i-Tree Manuals, Guides & Workbooks. Available online: <https://www.itreetools.org/support/resources-overview/i-tree-manuals-workbooks> (accessed on 1 July 2024).
31. David, J. *Nowak Assessing the Benefits and Economic Values of Trees*, 1st ed.; Routledge: London, UK, 2017.
32. Amini Parsa, V.; Salehi, E.; Yavari, A.R.; van Bodegom, P.M. Analyzing Temporal Changes in Urban Forest Structure and the Effect on Air Quality Improvement. *Sustain. Cities Soc.* **2019**, *48*, 101548. [[CrossRef](#)]
33. Cimburova, Z.; Barton, D.N. The Potential of Geospatial Analysis and Bayesian Networks to Enable I-Tree Eco Assessment of Existing Tree Inventories. *Urban. For. Urban. Green.* **2020**, *55*, 126801. [[CrossRef](#)]
34. Jia, X.; Han, H.; Feng, Y.; Song, P.; He, R.; Liu, Y.; Wang, P.; Zhang, K.; Du, C.; Ge, S.; et al. Scale-Dependent and Driving Relationships between Spatial Features and Carbon Storage and Sequestration in an Urban Park of Zhengzhou, China. *Sci. Total Environ.* **2023**, *894*, 164916. [[CrossRef](#)]
35. Feng, Y.; Zhang, K.; Li, A.; Zhang, Y.; Wang, K.; Guo, N.; Wan, H.Y.; Tan, X.; Dong, N.; Xu, X.; et al. Spatial and Seasonal Variation and the Driving Mechanism of the Thermal Effects of Urban Park Green Spaces in Zhengzhou, China. *Land* **2024**, *13*, 1474. [[CrossRef](#)]
36. Zhou, Z.X.; Li, J. The Correlation Analysis on the Landscape Pattern Index and Hydrological Processes in the Yanhe Watershed, China. *J. Hydrol.* **2015**, *524*, 417–426. [[CrossRef](#)]
37. Li, Q.; Zhou, Y.; Wang, L.; Zuo, Q.; Yi, S.; Liu, J.; Su, X.; Xu, T.; Jiang, Y. The Link between Landscape Characteristics and Soil Losses Rates over a Range of Spatiotemporal Scales: Hubei Province, China. *Int. J. Environ. Res. Public Health* **2021**, *18*, 11044. [[CrossRef](#)] [[PubMed](#)]
38. Lu, G.Q. Study on the Ecological Benefit Evaluation and the Dynamics Simulation About Urban Forest in Dalian. Ph.D. Thesis, Beijing Forestry University, Beijing, China, 2006.
39. Shi, Y. Vegetation Structure Characteristics and Carbon Uptake of Urban Built-Up Area in China. Ph.D. Thesis, Zhejiang University, Hangzhou, China, 2013.
40. Gao, H. Study on the Value of Green Space System Services of Manduhai Park. Master’s Thesis, Inner Mongolia Agricultural University, Hohhot, China, 2006.
41. Lian, J. The Structure and Benefits of Urban Forest in Xi’an City. Master’s Thesis, Northeast University, Xi’an, China, 2008.
42. Chen, W.Y. The Role of Urban Green Infrastructure in Offsetting Carbon Emissions in 35 Major Chinese Cities: A Nationwide Estimate. *Cities* **2015**, *44*, 112–120. [[CrossRef](#)]
43. Gao, S. Carbon Balance and Nutrient Cycle of Urban Forest in Changsha. Ph.D. Thesis, Central South University of Forestry and Technology, Changsha, China, 2010.
44. Shen, W.; Cui, X. Impact of Electric Vehicles and Renewable Energy Systems on Cost and Emission of Electricity. In Proceedings of the 2012 7th IEEE Conference on Industrial Electronics and Applications (ICIEA), Singapore, 18–20 July 2012; IEEE: Singapore, 2012; pp. 120–125.
45. Chen, S.; Liu, X.; Yang, L.; Zhu, Z. Variations in Ecosystem Service Value and Its Driving Factors in the Nanjing Metropolitan Area of China. *Forests* **2023**, *14*, 113. [[CrossRef](#)]
46. Pasher, J.; McGovern, M.; Khoury, M.; Duffe, J. Assessing Carbon Storage and Sequestration by Canada’s Urban Forests Using High Resolution Earth Observation Data. *Urban. For. Urban. Green.* **2014**, *13*, 484–494. [[CrossRef](#)]
47. Nowak, D.J.; Greenfield, E.J.; Hoehn, R.E.; Lapoint, E. Carbon Storage and Sequestration by Trees in Urban and Community Areas of the United States. *Environ. Pollut.* **2013**, *178*, 229–236. [[CrossRef](#)] [[PubMed](#)]
48. Jo, H. Impacts of Urban Greenspace on Offsetting Carbon Emissions for Middle Korea. *J. Environ. Manag.* **2002**, *64*, 115–126. [[CrossRef](#)]
49. Zhou, W.; Wang, J.; Qian, Y.; Pickett, S.T.A.; Li, W.; Han, L. The Rapid but “Invisible” Changes in Urban Greenspace: A Comparative Study of Nine Chinese Cities. *Sci. Total Environ.* **2018**, *627*, 1572–1584. [[CrossRef](#)] [[PubMed](#)]
50. Hong, W.; Ren, Z.; Guo, Y.; Wang, C.; Cao, F.; Zhang, P.; Hong, S.; Ma, Z. The Rapid but “Invisible” Changes in Urban Greenspace: A Comparative Study of Nine Chinese Cities. *Ecol. Indic.* **2024**, *159*, 111601. [[CrossRef](#)]
51. Rui, Z.S.T. The influence of landscape characteristics of a park green space on the park cool island effect in Zhengzhou City. *Ecol. Lett.* **2020**, *40*, 2886–2894. [[CrossRef](#)]

52. Cai, G.; Lin, Y.; Zhang, F.; Zhang, S.; Wen, L.; Li, B. Response of Ecosystem Service Value to Landscape Pattern Changes under Low-Carbon Scenario: A Case Study of Fujian Coastal Areas. *Land* **2022**, *11*, 2333. [[CrossRef](#)]
53. Guo, M.; Chen, S.; Zhang, Y. Spatial Analysis on the Role of Multi-Dimensional Urbanizations in Carbon Emissions: Evidence from China. *Int. J. Environ. Res. Public Health* **2022**, *19*, 5315. [[CrossRef](#)] [[PubMed](#)]
54. Wang, H.; Feng, Y.; Ai, L. Progress of Carbon Sequestration in Urban Green Space Based on Bibliometric Analysis. *Front. Environ. Sci.* **2023**, *11*, 1196803. [[CrossRef](#)]
55. Wang, R.-Y.; Mo, X.; Ji, H.; Zhu, Z.; Wang, Y.-S.; Bao, Z.; Li, T. Comparison of the CASA and InVEST Models' Effects for Estimating Spatiotemporal Differences in Carbon Storage of Green Spaces in Megacities. *Sci. Rep.* **2024**, *14*, 5456. [[CrossRef](#)] [[PubMed](#)]
56. Chen, M.; Jia, W.; Du, C.; Shi, M.; Henebry, G.M.; Wang, K. Carbon Saving Potential of Urban Parks Due to Heat Mitigation in Yangtze River Economic Belt. *J. Clean. Prod.* **2023**, *385*, 135713. [[CrossRef](#)]
57. Song, J.; Zhang, R.; Wang, Y.; Huang, J. Evolution Characteristics of Wetland Landscape Pattern and Its Impact on Carbon Sequestration in Wuhan from 2000 to 2020. *Land* **2023**, *12*, 582. [[CrossRef](#)]
58. Gao, J.; Han, H.; Ge, S. Carbon-Saving Potential of Urban Parks in the Central Plains City: A High Spatial Resolution Study Using a Forest City, Shangqiu, China, as a Lens. *Land* **2023**, *12*, 1383. [[CrossRef](#)]
59. Park, H.-M.; Jo, H.-K.; Kim, J.-Y. Carbon Footprint of Landscape Tree Production in Korea. *Sustainability* **2021**, *13*, 5915. [[CrossRef](#)]
60. Tang, Z.; Wang, Y.; Fu, M.; Xue, J. The Role of Land Use Landscape Patterns in the Carbon Emission Reduction: Empirical Evidence from China. *Ecol. Indic.* **2023**, *156*, 111176. [[CrossRef](#)]
61. Whittinghill, L.J.; Rowe, D.B.; Schutzki, R.; Cregg, B.M. Quantifying Carbon Sequestration of Various Green Roof and Ornamental Landscape Systems. *Landsc. Urban. Plan.* **2014**, *123*, 41–48. [[CrossRef](#)]
62. Jung, M.C. Urban Landscape Affects Scaling of Transportation Carbon Emissions across Geographic Scales. *Sustain. Cities Soc.* **2024**, *113*, 105656. [[CrossRef](#)]
63. Hou, Y.; Wang, L.; Li, Z.; Ouyang, X.; Xiao, T.; Wang, H.; Li, W.; Nie, X. Landscape Fragmentation and Regularity Lead to Decreased Carbon Stocks in Basins: Evidence from Century-Scale Research. *J. Environ. Manag.* **2024**, *367*, 121937. [[CrossRef](#)] [[PubMed](#)]
64. Li, H. Dynamic Response of the Vegetation Carbon Storage in the Sanjiang Plain to Changes in Land Use/Cover and Climate. *Herit. Sci.* **2021**, *9*, 134. [[CrossRef](#)]
65. Tao, P.; Lin, Y.; Wang, X.; Li, J.; Ma, C.; Wang, Z.; Dong, X.; Yao, P.; Shao, M. Optimization of Green Spaces in Plain Urban Areas to Enhance Carbon Sequestration. *Land* **2023**, *12*, 1218. [[CrossRef](#)]
66. Brinck, K.; Fischer, R.; Groeneveld, J.; Lehmann, S.; Dantas De Paula, M.; Pütz, S.; Sexton, J.O.; Song, D.; Huth, A. High Resolution Analysis of Tropical Forest Fragmentation and Its Impact on the Global Carbon Cycle. *Nat. Commun.* **2017**, *8*, 14855. [[CrossRef](#)]
67. Dang, H. Multi-Scenario Simulation Can Contribute to Identify Priorities for Regional Ecological Corridors Conservation. *Ecol. Indic.* **2024**, *165*, 112166. [[CrossRef](#)]
68. Carbon Stock Corridors to Mitigate Climate Change and Promote Biodiversity in the Tropics | Nature Climate Change. Available online: <https://www.nature.com/articles/nclimate2105> (accessed on 17 August 2024).
69. Moomaw, W.R. Wetlands In a Changing Climate: Science, Policy and Management. *Wetlands* **2018**, *38*, 183–205. [[CrossRef](#)]
70. Nahlik, A.M.; Fennessy, M.S. Carbon Storage in US Wetlands. *Nat. Commun.* **2016**, *7*, 13835. [[CrossRef](#)]
71. Fortier, J.; Truax, B.; Gagnon, D.; Lambert, F. Biomass Carbon, Nitrogen and Phosphorus Stocks in Hybrid Poplar Buffers, Herbaceous Buffers and Natural Woodlots in the Riparian Zone on Agricultural Land. *J. Environ. Manag.* **2015**, *154*, 333–345. [[CrossRef](#)]
72. Liu, Y.; Fan, C.; Xue, D. A Review of the Effects of Urban and Green Space Forms on the Carbon Budget Using a Landscape Sustainability Framework. *Sustainability* **2024**, *16*, 1870. [[CrossRef](#)]
73. Han, J.; Meng, X.; Zhou, X.; Yi, B.; Liu, M.; Xiang, W.-N. A Long-Term Analysis of Urbanization Process, Landscape Change, and Carbon Sources and Sinks: A Case Study in China's Yangtze River Delta Region. *J. Clean. Prod.* **2017**, *141*, 1040–1050. [[CrossRef](#)]
74. Sha, Z.; Bai, Y.; Li, R.; Lan, H.; Zhang, X.; Li, J.; Liu, X.; Chang, S.; Xie, Y. The Global Carbon Sink Potential of Terrestrial Vegetation Can Be Increased Substantially by Optimal Land Management. *Commun. Earth Env.* **2022**, *3*, 8. [[CrossRef](#)]

Disclaimer/Publisher's Note: The statements, opinions and data contained in all publications are solely those of the individual author(s) and contributor(s) and not of MDPI and/or the editor(s). MDPI and/or the editor(s) disclaim responsibility for any injury to people or property resulting from any ideas, methods, instructions or products referred to in the content.